

Autosomal-dominant polycystic kidney disease in the rat

BENJAMIN D. COWLEY, JR., SESHAGIRIRAO GUDAPATY, AMY L. KRAYBILL,
BRIAN D. BARASH, MICHAEL A. HARDING, JAMES P. CALVET, and VINCENT H. GATTONE, II

Departments of Anatomy and Cell Biology, Medicine, and Biochemistry and Molecular Biology, The University of Kansas Medical Center, Kansas City, Kansas, USA

Autosomal-dominant polycystic kidney disease in the rat. Kaspereit-Rittinghausen described a rodent model of inherited polycystic kidney disease (PKD), the Han:SPRD rat [1, 2], in which heterozygotes develop renal cysts and renal failure (in males) over several months, whereas homozygous animals develop rapidly progressive renal enlargement that leads to death in a few weeks. In this study, we examined selected elements of the pathogenesis of this disease in heterozygotes and homozygotes from birth to advanced disease. Heterozygous male rats developed slowly progressive renal cystic disease with interstitial fibrosis and azotemia seen by six months of age. Female heterozygotes developed slowly progressive renal cystic disease, but did not develop interstitial fibrosis or azotemia. Epithelial cells lining cyst cavities showed various degrees of morphologic immaturity. Cyst walls also developed basement membrane thickening, especially in areas of cellular immaturity, suggesting an interrelationship between this basement membrane thickening and cellular dedifferentiation. Thickened basement membranes were associated with increased immunoreactivity for type IV collagen, laminin, and fibronectin. Homozygous rats developed massive renal enlargement, marked azotemia, and died near three weeks of age. Renal *c-myc* proto-oncogene expression was elevated in homozygous cystic infants and in adult heterozygotes. *In situ* hybridization showed high levels of *c-myc* mRNA in cyst epithelia, suggesting abnormal regulation of cellular proliferation in the cells lining cysts, as seen in other models of PKD. The Han:SPRD rat is the only well-documented animal model of inherited PKD with an autosomal-dominant inheritance pattern and appears to have several features which resemble human ADPKD.

Hereditary forms of polycystic kidney disease (PKD) in humans are transmitted in either an autosomal recessive (ARPKD) or an autosomal dominant pattern (ADPKD). ARPKD is rare (incidence = 1/6,000 to 14,000 live births) and usually fatal in infancy, although affected individuals occasionally survive into early adulthood [3]. ADPKD is relatively common, affecting approximately half a million people in the United States alone. ADPKD usually progresses slowly with approximately 50% of affected individuals developing renal failure by the fifth decade [3]. While several genetic models for the infantile form of PKD exist, progress in understanding the pathogenesis of ADPKD has been hindered by the lack of a suitable animal model. A murine model of slowly progressive PKD, the DBA-*pcy*, was described recently, however, the disease is transmitted as an autosomal recessive trait [4].

In 1989, Kaspereit-Rittinghausen described a strain of rats, the Han:SPRD, that inherited PKD as an autosomal dominant trait [1, 2]. The pathologic features, reported in preliminary detail, were consistent with a polycystic kidney disease comparable to that seen in humans. The present study characterizes further the polycystic kidney disease in the Han:SPRD rat including renal histologic features associated with the development of cystic disease and azotemia, proto-oncogene expression, and alterations of the extracellular matrix. Heterozygous Han:SPRD rats developed chronic progressive azotemia (the severity of which was affected by gender), renal tubular basement membrane abnormalities, and morphologic and molecular evidence of abnormal cellular proliferation. These findings suggest that the Han:SPRD rat will be a useful model for studies of the pathogenesis and treatment of inherited renal cystic disease.

Methods

Animals

A litter of Han:SPRD rats (abnormal gene designated Cy), the offspring of two heterozygous Cy/+ rats, was provided by Dr. Kaspereit-Rittinghausen and used for the development of a breeding colony, which was maintained in the Animal Care Facility at The University of Kansas Medical Center. Inquiries concerning the Han:SPRD rats used in these studies should be addressed to Dr. Cowley.

As previously reported [1, 2], homozygous Cy/Cy rats developed massively enlarged kidneys (Fig. 1) and severe azotemia (Fig. 2), and died at approximately three weeks of age. Homozygotes of either sex are easily identified after approximately one week of age by abdominal palpation, a finding used to verify parental heterozygosity for PKD. Thus, heterozygote breeders used to maintain successive generations of the colony were identified by test breeding sibling offspring of heterozygous parents. Rats had free access to standard rat chow and tap water. Male and female rats of the three genotypes (Cy/Cy, Cy/+, +/+) were studied at newborn, 1, 2, and 3 weeks of age; Cy/+ and +/+ rats were also studied at 8, 24, and 44 weeks of age. A total of 181 animals were examined.

At the time of sacrifice, rats were anesthetized with sodium pentobarbital (50 mg/kg, i.p.) and weighed. Blood was obtained (from the heart or inferior vena cava), and the right kidney was removed, weighed, and immediately processed for RNA isolation (*v.i.*). The left kidney was perfusion-fixed with 4%

Received for publication July 2, 1992
and in revised form October 13, 1992
Accepted for publication October 15, 1992

© 1993 by the International Society of Nephrology

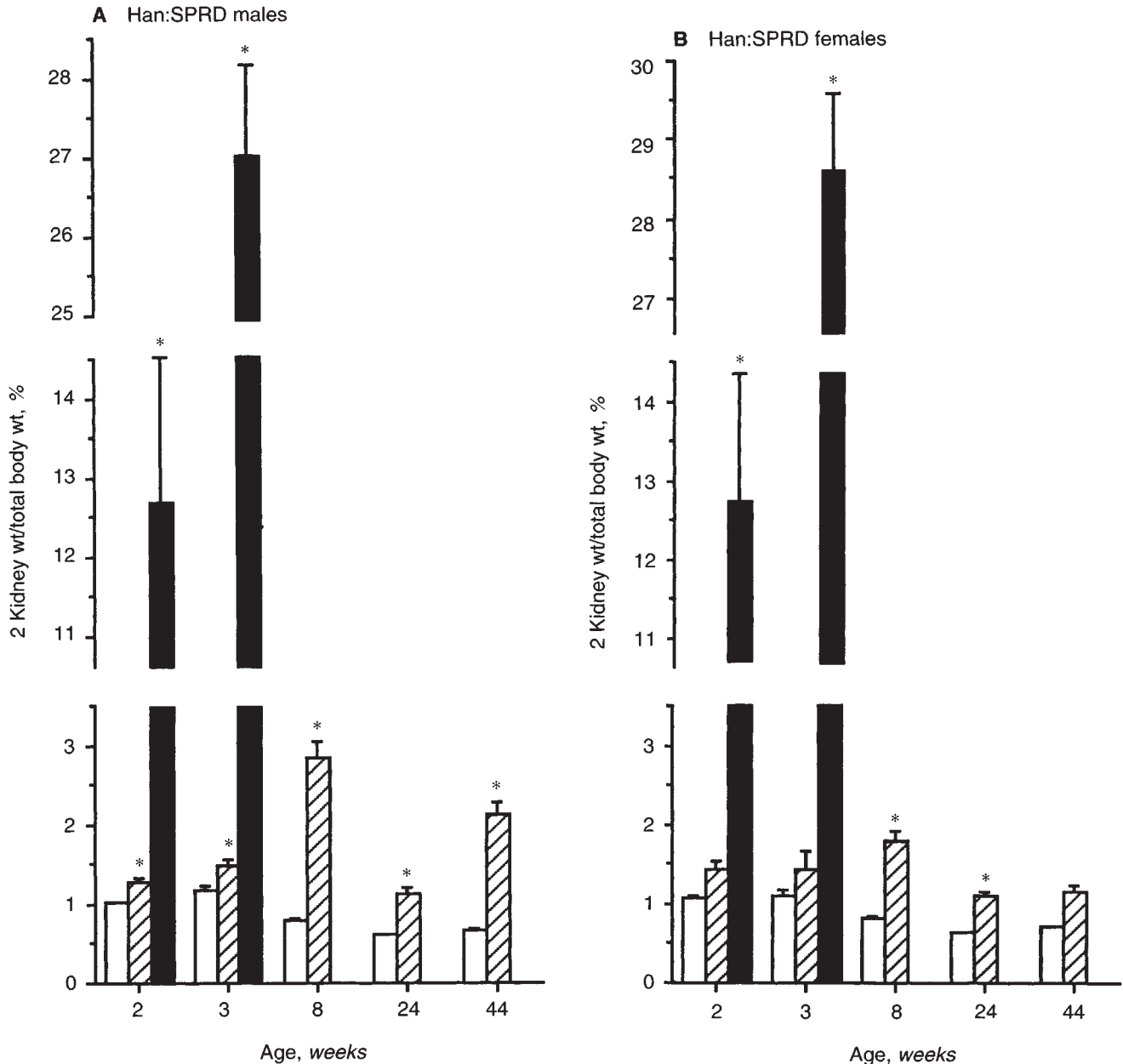


Fig. 1. Kidney weight as a percent of total body weight in male (A) and female (B) Han:SPRD rats. Values are means \pm SEM. Symbols are: (\square) +/+; (\square with diagonal lines) Cy/+; (\blacksquare) Cy/Cy. Numbers of animals represented (+/+, Cy/+, Cy/Cy) are: males, 2 week old (4, 5, 4), 3 week old (7, 6, 2), 8 week old (7, 7, —), 24 week old (8, 12, —), 44 week old (4, 12, —); females, 2 week old (5, 6, 5), 3 week old (5, 2, 2), 8 week old (3, 9, —), 24 week old (7, 13, —), 44 week old (1, 5, —). * $P < 0.01$.

paraformaldehyde in 0.1 M phosphate buffered saline or 2.5% glutaraldehyde in 0.1 M cacodylate buffer and weighed.

Serum samples were analyzed for urea nitrogen level using a colorimetric method (Sigma Kit # 640-B, Sigma Chemical Co., St. Louis, Missouri, USA). Total kidney weight was expressed as a percent of body weight to compensate for growth retardation associated with azotemia in suckling animals. Serum urea nitrogen and kidney weight data were statistically analyzed by unpaired *t*-test when only two groups were compared. When three groups were compared, data were analyzed by one way analysis of variance. When differences were detected, groups

were analyzed by pairwise *t*-tests between groups, controlling for type I error by adjusting the level of significance by the Bonferroni procedure.

Renal histopathology

For light microscopy, portions of paraformaldehyde-fixed kidneys were paraffin embedded, sectioned onto glass slides, and stained with hematoxylin and eosin (H&E), periodic acid Schiff's reaction (PAS), or picrosirius red (PR). Sections were examined and photographed using a Nikon Labophot microscope (Nikon, Melville, New York, USA).

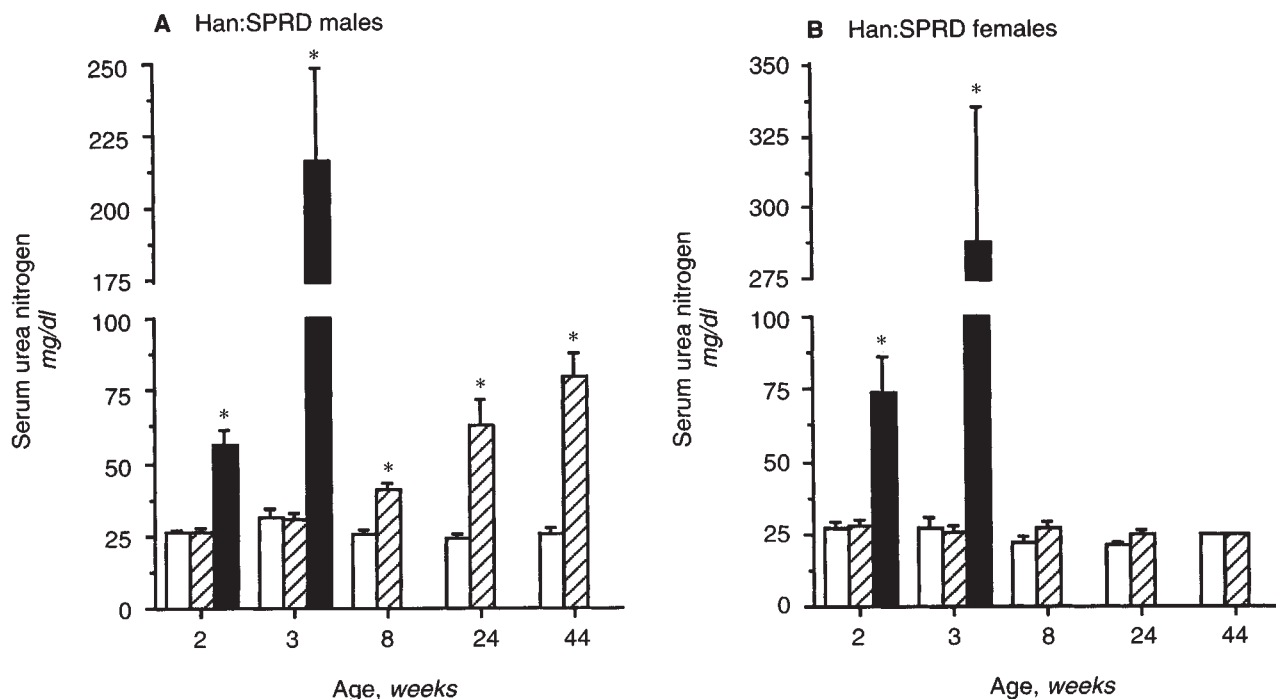


Fig. 2. Serum urea nitrogen in male (A) and female (B) Han:SPRD rats. Values are means \pm SEM. Symbols are: (□) +/+; (▨) Cy/+; (■) Cy/Cy. Numbers of animals represented (+/+, Cy/+, Cy/Cy) are: males, 2 week old (4, 5, 4), 3 week old (4, 5, 3), 8 week old (7, 11, —), 24 week old (8, 12, —), 44 week old (4, 12, —); females, 2 week old (5, 6, 5), 3 week old (3, 4, 3), 8 week old (4, 10, —), 24 week old (7, 13, —), 44 week old (1, 5, —). * $P < 0.01$.

For immunohistochemistry, portions of paraformaldehyde-fixed kidneys were frozen in liquid nitrogen and stored at -70°C until use. Frozen sections of these kidneys were placed onto chrome-alum subbed slides and examined using standard indirect immunofluorescence methods. Sections were rinsed in PBS with normal goat serum prior to incubation with primary antisera against laminin, type IV collagen, or fibronectin (Chemicon Int., Inc., Temecula, California, USA) (antisera dilutions = 1:200, 1:320, and 1:100, respectively) for 18 hours at room temperature. Slides were rinsed with PBS, and the secondary antibody, conjugated with either lisamine rhodamine or fluorescein (Jackson Immuno Research Lab, Inc., West Grove, Pennsylvania, USA), was incubated with the sections for one hour at room temperature. Sections were examined and photographed using a Nikon Biophot microscope equipped for epifluorescence.

For electron microscopy (EM), sections of glutaraldehyde-fixed kidneys were rinsed in cacodylate buffer, placed in 1% OsO_4 , and then dehydrated using increasing concentrations of ethanol. For scanning EM (SEM), the tissue was critical point dried, sputter coated with gold, and examined using a JEOL scanning electron microscope (JEOL USA, Inc., Peabody, Massachusetts, USA). For transmission EM (TEM), tissue was embedded in LX112 resin (Ladd Research, Inc., Burlington, Vermont, USA) and sectioned. Thin sections (100 nm) were stained with lead citrate and uranyl acetate and examined using a JEOL transmission electron microscope.

RNA isolation

RNA was isolated from right kidneys essentially as described by Chomczynski and Sacchi [5]. Briefly, right kidneys were

homogenized in GTC solution (4 M guanidine thiocyanate, 25 mM sodium citrate, 100 mM 2-mercaptoethanol, 0.1% Antifoam A, pH 7). Subsequently 0.1 volume 2 M sodium acetate, pH 4.0, 1 volume phenol, and 0.2 volumes chloroform were serially added with vortexing between each addition. Samples were chilled on ice ≥ 15 minutes and then centrifuged at $6650 \times g$ for 10 minutes. The aqueous phase was recovered, 1 volume of isopropanol was added, and samples were stored at -20°C overnight. RNA was pelleted by centrifugation at $6650 \times g$ for 20 minutes, the supernatant was discarded, and RNA was redissolved in TES (10 mM TRIS, 2 mM EDTA, 0.1% SDS, pH 7). Samples were chloroform extracted, and the RNA was precipitated by addition of 0.1 volumes 3 M sodium acetate, pH 5.2 and 2.5 volumes 95% ethanol and pelleted by centrifugation at $9000 \times g$ for 30 minutes. RNA was redissolved in TES and quantitated by spectrophotometry. RNA was then precipitated by addition of 0.1 volumes 3 M sodium acetate, pH 5.2 and 2.5 volumes 95% ethanol, and RNA samples were stored at -20°C until use.

Denaturing gels and Northern transfers

RNA samples (equal amounts per lane) were denatured in 2.2 M formaldehyde, 50% formamide and electrophoresed in 2.2 M formaldehyde, 1.0% agarose gels. Gels were stained with acridine orange and photographed prior to blot transfer in order to locate the 18S and 28S ribosomal RNA bands and to confirm loading of equal amounts of RNA in each lane. RNA was transferred to Nytran membranes (Schleicher & Schuell, Keene, New Hampshire, USA) according to Thomas [6]. Filters were then baked *in vacuo* at 80°C for four hours.

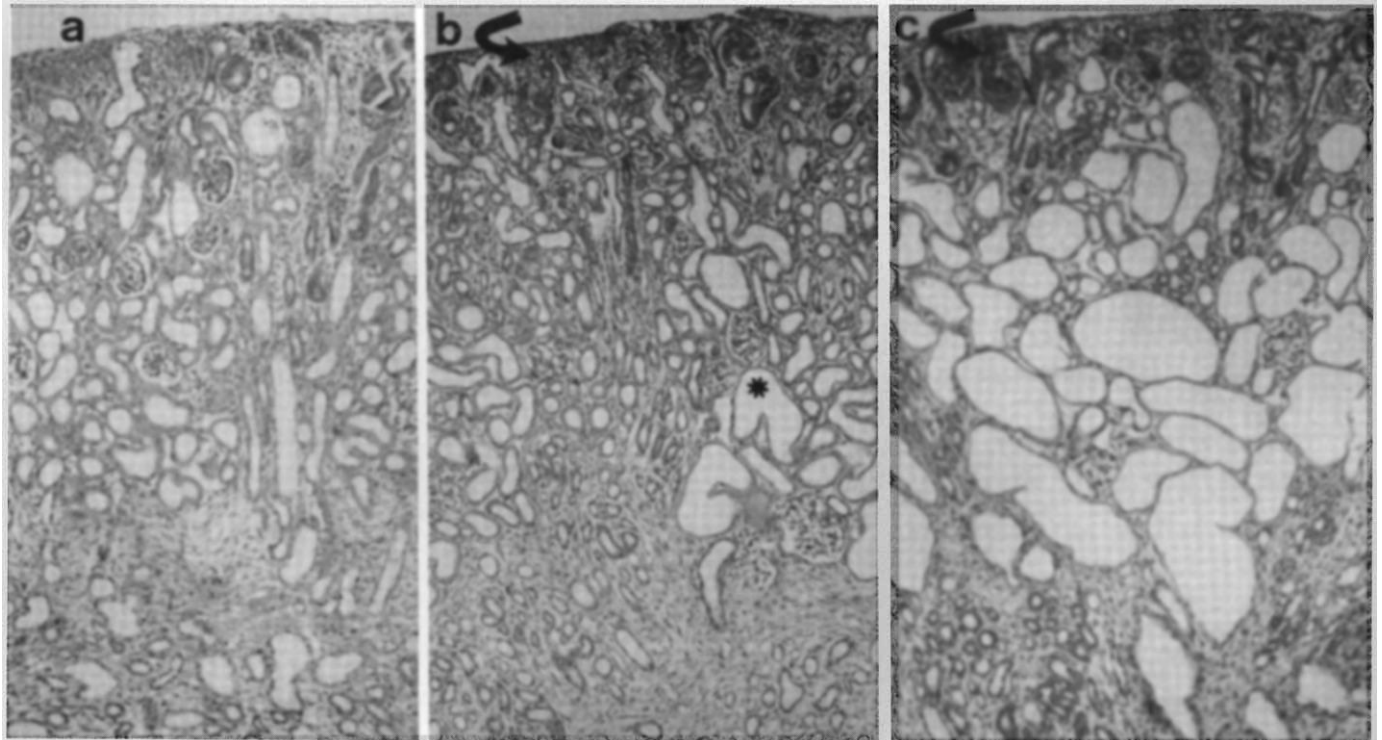


Fig. 3. Light micrograph of kidneys from newborn normal $+/+$ rats (a), heterozygous $Cy/+$ rats (b), and homozygous Cy/Cy cystic (c) rats. The nephrogenic zone of $Cy/+$ and Cy/Cy rats (arrows) is unaffected. Virtually all cortical tubules are dilated in Cy/Cy rats. A few inner cortical proximal tubules, as well as some distal tubules and collecting ducts, are dilated in the $Cy/+$ rat. There was no significant histopathologic difference in the disease exhibited by males and females at this age; these micrographs are from a male (a), a female (b), and a male (c). All photographs are at the same magnification ($110\times$).

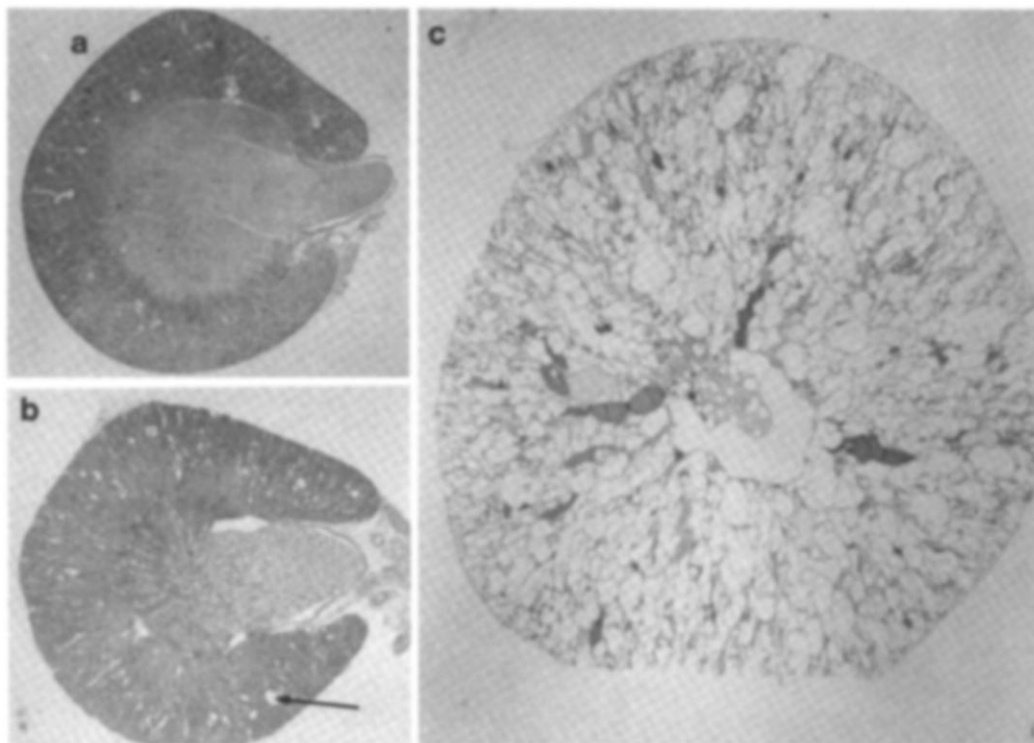


Fig. 4. Light micrographs of kidneys from 3-week-old normal $+/+$ rats (a), heterozygous $Cy/+$ rats (b), and homozygous Cy/Cy cystic (c) rats. The heterozygous $Cy/+$ kidney exhibits several inner cortical, proximal tubular cysts (arrow). The kidney of the homozygous Cy/Cy cystic rat is massively enlarged by innumerable renal cysts throughout the cortex and outer medulla. No normal appearing renal parenchyma remains at this stage of the cystic disease in the Cy/Cy rat. Once again, there was no significant histopathologic difference in the disease exhibited by males and females at this age; these micrographs are from a female (a), a female (b), and a male (c). All photographs are at the same magnification ($7\times$).

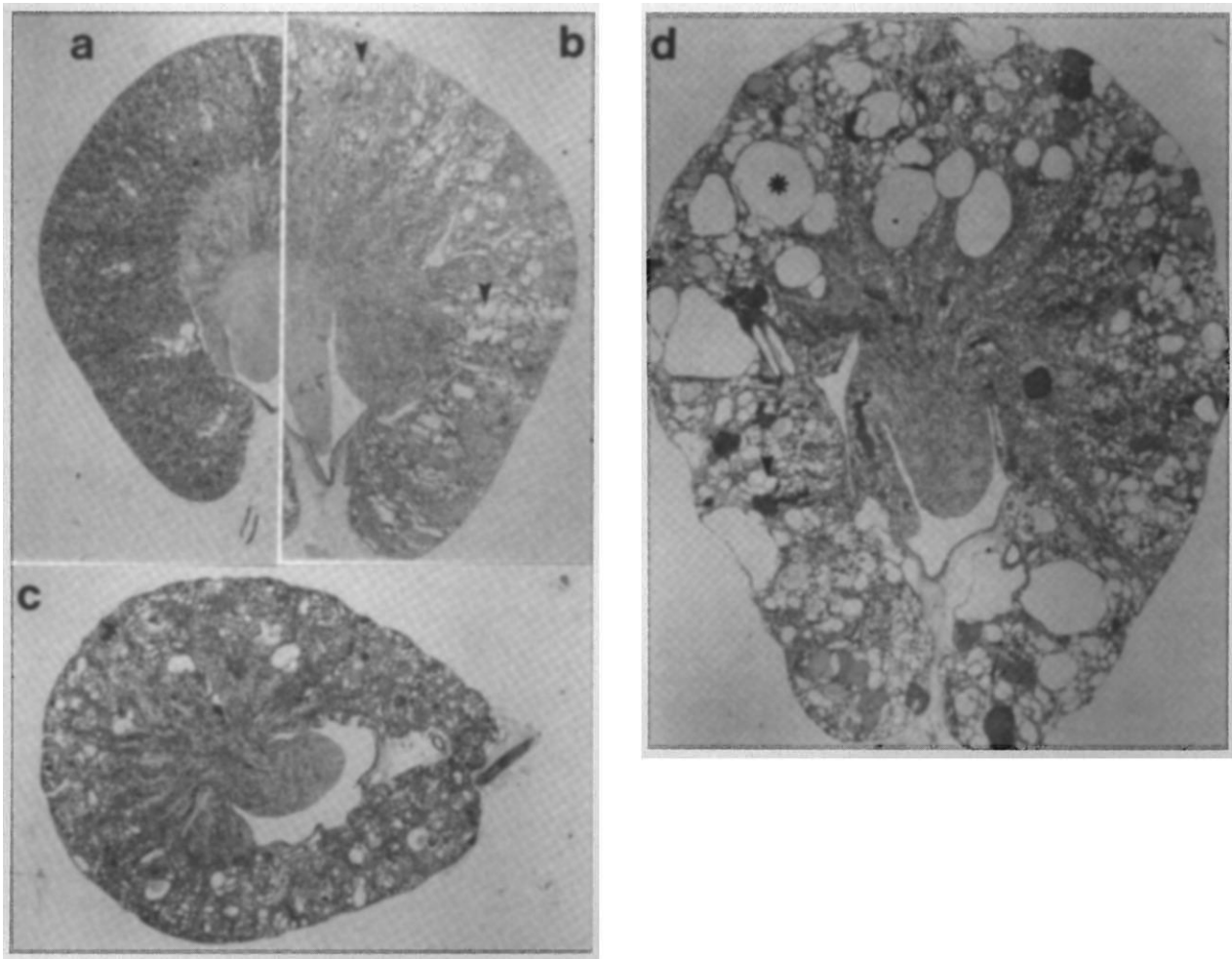


Fig. 5. Light micrograph of kidneys from male *Han:SPRD* rats: (a) normal $+/+$ 10 week old, (b) heterozygous *Cy/+* 10 week old, (c) heterozygous *Cy/+* 24 week old, (d) heterozygous *Cy/+* 44 week old. The numerous small inner cortical cysts in the 10 week old *Cy/+* (arrowheads) largely regressed by 24 weeks, however numerous very large cysts (asterisk), as well as small cysts (arrowheads), developed by 44 weeks. All photographs are at the same magnification ($5\times$).

RNA hybridizations

Filters to be probed for *c-myc* were prehybridized at 66°C in $3\times$ SET ($20\times$ SET is 3 M NaCl, 0.04 M EDTA, 0.6 M Tris HCl, pH 8), 0.1% SDS, $10\times$ Denhardt's solution ($10\times$ Denhardt's solution is 0.2% Ficoll, 0.2% polyvinylpyrrolidone, 0.2% bovine serum albumin), 250 μg of tRNA per ml for two hours or longer. Hybridizations were carried out overnight at 66°C in $3\times$ SET, 0.1% SDS, 20 mM sodium phosphate buffer, pH 7.8, $10\times$ Denhardt's, 250 μg of tRNA per ml, 10% dextran sulfate, with 10^6 cpm of [^{32}P]-radiolabeled antisense RNA probe (*v.i.*) per ml of hybridization solution. Filters were washed at 66°C in $1\times$ SSC ($20\times$ SSC is 3 M NaCl, 0.3 M trisodium citrate, pH 7), 0.1% SDS for one hour, $0.3\times$ SSC, 0.1% SDS for one hour, and $0.1\times$ SSC, 0.1% SDS for one hour. Filters were then exposed to Kodak XAR film at -80°C .

Results presented are representative of multiple experiments. The following is a summary of the number of experiments performed with age, gender, number of litters examined, number of animals examined, and number of blots performed: two week old male: one litter, (4 $+/+$, 2 *Cy/+*, 1 *Cy/Cy*), six blots; two week old female: one litter, (2 $+/+$, 2 *Cy/+*, 2 *Cy/Cy*), six

blots; three week old male: two litters, (2 $+/+$, 2 *Cy/+*, 3 *Cy/Cy*), six blots; three week old female: two litters, (3 $+/+$, 2 *Cy/+*, 3 *Cy/Cy*), six blots; eight week old male: two litters, (5 $+/+$, 4 *Cy/+*), six blots; eight week old female: three litters, (3 $+/+$, 6 *Cy/+*), six blots; 24 week old male: two litters, (4 $+/+$, 5 *Cy/+*), six blots; 24 week old female: one litter, (1 $+/+$, 3 *Cy/+*), three blots. Densitometry of all autoradiographs was performed using a Fisher Biotec model FB910 scanning densitometer.

Generation of antisense RNA probes

Transcriptions for generation of radiolabeled anti-sense RNA probes specific for *c-myc* were performed as previously described [7]. The plasmid used for generation of probes was pc-myc, containing a Hind III/Sac I fragment from exons 2 and 3 of mouse *c-myc* subcloned into pSP64. This plasmid was linearized with Pvu II prior to transcription. Radiolabeled antisense RNA probes were prepared by *in vitro* transcription using SP6 RNA polymerase (Promega, Madison, Wisconsin,

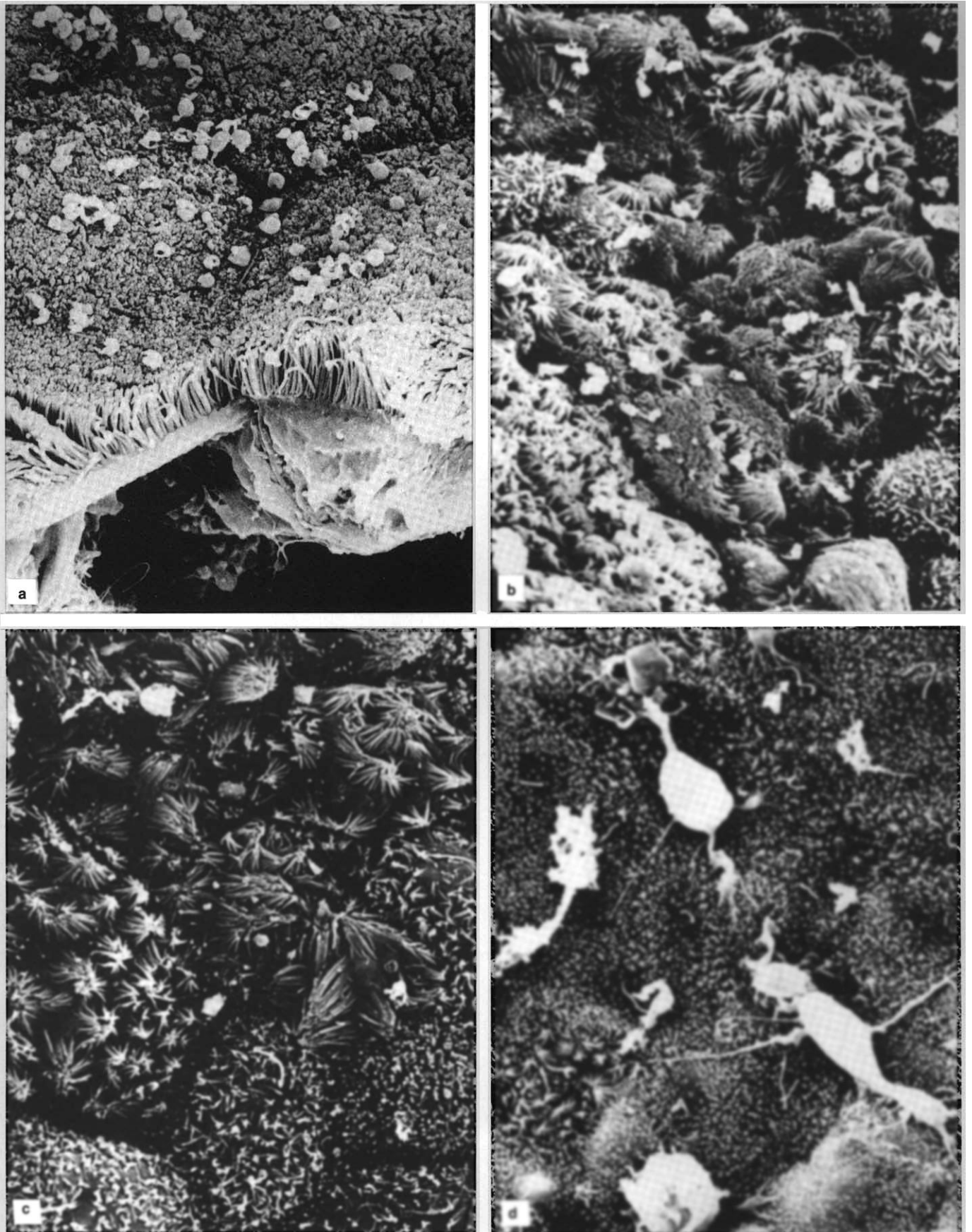


Fig. 6. *Scanning electron micrographs of cells lining proximal tubular cysts. Cellular phenotype varied within a single cyst. Compared to normal proximal tubule (a), the epithelia from much of the cyst walls exhibited various stages of cellular dedifferentiation (e.g., rarefaction of microvilli) (b-d). (Magnifications: a 5,900 \times , b 2,000 \times , c 2,660 \times , d 2,130 \times).*

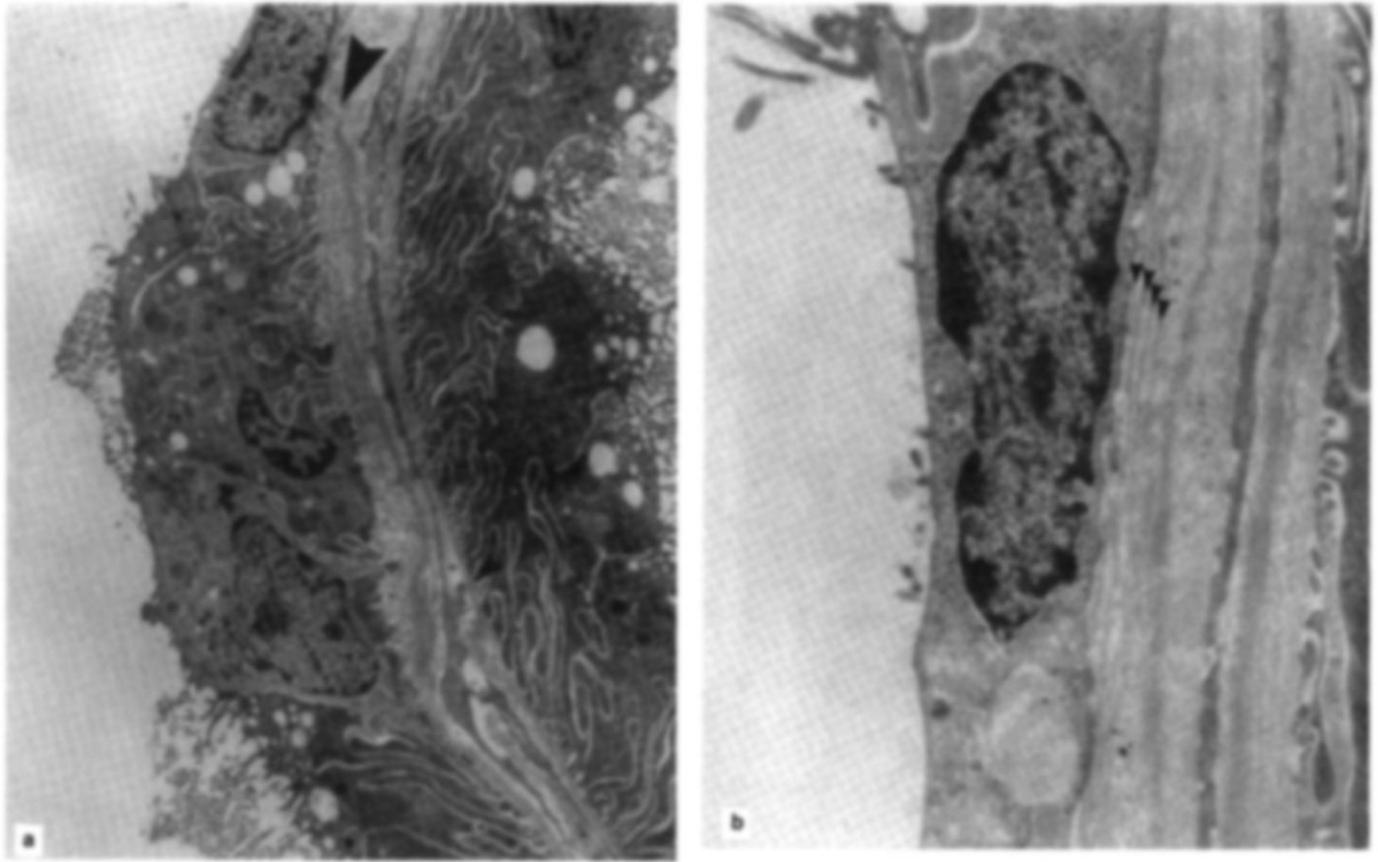


Fig. 7. Transmission electron micrographs of epithelia lining proximal tubular cysts. (a) A mixture of cellular phenotypes was seen, with some cells showing loss of microvilli and reduced basolateral infoldings by the plasmalemma. The basement membrane underlying these dedifferentiated cells was greatly thickened (large arrowhead) compared to more normal appearing basement membrane underlying phenotypically normal proximal tubular cells (small arrowhead). (b) The basement membrane thickening often had a multilaminated appearance (arrowheads). (Magnifications: a 4,000 \times , b 13,000 \times).

USA) and linearized plasmid in the presence of α -[^{32}P]-guanosine triphosphate or α -[^{35}S]-guanosine triphosphate (DuPont/NEN, Wilmington, Delaware, USA).

In situ hybridizations

The methods for *in situ* hybridization have been adapted from those published elsewhere [8, 9]. Rats were anesthetized with sodium pentobarbital and their kidneys were perfusion-fixed with 4% paraformaldehyde in phosphate-buffered saline (PBS) followed by immersion in the same fixative. Pieces of kidney were cryoprotected by soaking in 15% sucrose/PBS then embedded in O.C.T. compound (Miles Scientific, Naperville, Illinois, USA) and snap-frozen in liquid nitrogen. Eight micrometer sections were mounted on poly-L-lysine coated slides and fixed an additional 15 minutes in 4% paraformaldehyde/PBS. After rinsing in PBS, slides were acetylated, washed in 2 \times SSC, and dehydrated in ethanol. Sections were incubated first in 5 mM MgCl_2 /PBS and then in 0.25 M Tris, 0.1 M glycine, pH 7. A wash of 50% formamide, 2 \times SET was carried out at 37°C for 10 minutes. Hybridization solution, containing 2 \times SET, 10 \times Denhardt's solution, 250 $\mu\text{g}/\text{ml}$ yeast tRNA, 50% formamide, 0.1 M DTT, 10% dextran sulfate, and approximately 0.05 mg/ml of ^{35}S -labeled antisense RNA probe, was placed on the sections. Sections were then covered with a siliconized coverslip and immersed in paraffin oil. Hybridization took place

overnight at 45°C. Excess paraffin oil was removed by washing in chloroform, and coverslips were removed by soaking in 4 \times SSC. Slides were washed in 50% formamide, 2 \times SET, 10 mM DTT for 15 minutes at 60°C, then incubated with RNase A (20 mg/ml RNase A, 3 \times SET, 100 mg/ml BSA) for 30 minutes at 37°C. After washing in 1 \times SSC at room temperature for 30 minutes, the slides were washed a final time in 0.2 \times SSC, 0.1% mercaptoethanol at 50°C for 30 minutes then dehydrated in ethanol. Autoradiography was performed with Kodak NTB-2 liquid emulsion. The sections were stained in hematoxylin and eosin following development.

Results

Renal enlargement and development of azotemia

The degree of renal enlargement in both male (Fig. 1A) and female (Fig. 1B) Han:SPRD rats was clearly affected by gene dose. Homozygous Cy/Cy rats (both male and female) showed significant renal enlargement from birth with such rapid renal growth that kidneys accounted for approximately 25% to 30% of total body weight by three weeks of age. Renal enlargement in Cy/Cy rats (Figs. 1A and B) correlated with the elevation of serum urea nitrogen (SUN) seen in these same animals (Figs. 2A and B).

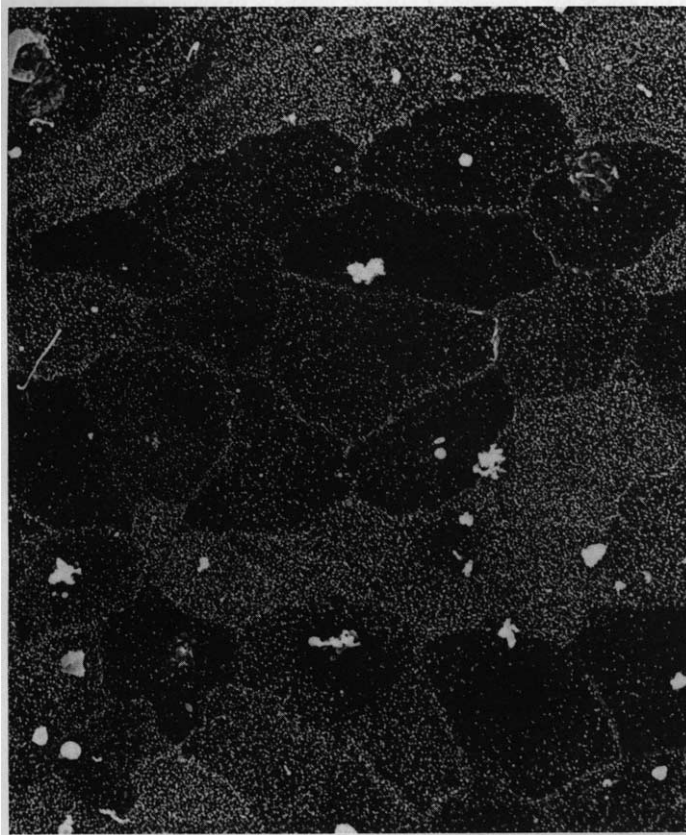


Fig. 8. Scanning electron micrograph of the epithelia lining a distal tubular cyst. Variability in the cellular phenotypes was seen in distal tubular cysts (for example, rarefaction of microvilli). (Magnification = 1,800 \times).

Cystic disease in heterozygous Cy/+ rats differed in males and females. In heterozygous Cy/+ males, renal enlargement was evident during the suckling period with continued enlargement until about 12 weeks of age (Fig. 1A; data not shown). Renal growth was greater in males than in females but never reached the proportional size seen in the Cy/Cy (Fig. 1). Male heterozygotes developed azotemia by eight weeks of age which was progressive thereafter (Fig. 2A), however, renal size regressed somewhat between 8 and 24 weeks of age (kidney weight \pm SEM at 8 weeks = 8.02 ± 0.59 g, kidney weight \pm SEM at 24 weeks = 4.83 ± 0.37 g; $P < 0.01$ by unpaired *t*-test). The cystic disease worsened between 24 and 44 weeks of age (Figs. 1A and 5), and azotemia became more severe (Fig. 2A) during this later stage of the disease.

In heterozygous Cy/+ females, renal enlargement was also evident until about 12 weeks of age (Fig. 1B; data not shown). Thereafter, kidney size regressed, as seen in male heterozygotes, but kidney size was stable in female heterozygotes between 24 and 44 weeks of age, in contrast to the renewed enlargement seen in older male heterozygotes (Fig. 1). Significant azotemia did not develop in female heterozygous Cy/+ rats (Fig. 2B).

Cystic enlargement of the kidney did not correlate well with the degree of azotemia in the heterozygous rat since (1) female heterozygotes developed minimal, if any, azotemia (Fig. 2B) in the presence of significant cystic change, and (2) male heterozy-

gotes had minimal azotemia during the period of greatest renal enlargement and cystic change (8 to 12 weeks of age), however, males did develop significant azotemia when renal enlargement was actually regressing (24 weeks of age).

Renal morphology

The morphologic changes in homozygous Cy/Cy rats consisted of cystic dilation of all nephron segments except those in the nephrogenic zone of young [newborn (Fig. 3c) through ~12 day old] pups, though cystic changes were less pronounced in the inner medulla. By three weeks the renal architecture was completely distorted by the innumerable cysts in the Cy/Cy rat, although cyst development was less aggressive in the inner medulla (Fig. 4c).

Renal cyst development was minimal in Cy/+ rats during this early period (Figs. 3b and 4b) and affected mainly the proximal tubules of juxtamedullary nephrons. By 8 to 10 weeks cysts were more prominent in Cy/+ rats (Fig. 5b) but still mainly affected proximal tubules of juxtamedullary nephrons. Males were more severely affected than females at this age. By 24 weeks (Fig. 5c) the actual amount of cystic change appeared to have regressed, consistent with the kidney weight data (Fig. 1A). By 44 weeks, kidneys of male Cy/+ rats had numerous macroscopic cysts (Fig. 5d), resulting in very large kidneys (Fig. 1A). Female Cy/+ rats never developed this later form of renal enlargement (Fig. 1B), prominent macroscopic cysts (data not shown), or significant azotemia (Fig. 2B).

Most of the cystic change in heterozygous Cy/+ rats appeared to start in the proximal tubules of the juxtamedullary nephrons, however, some distal nephron segments in the inner cortex were also cystic. The epithelia lining proximal tubule cysts in heterozygotes also had focal areas exhibiting an immature cellular phenotype [rarefaction of microvilli (Figs. 6 and 7), less prominent infoldings of basolateral membranes]. Cells lining some distal tubule cysts also showed variability in the apical microvillar density (Fig. 8).

Prominent thickening of the basement membrane was closely associated with the areas of epithelial immaturity in heterozygous Cy/+ rats (Fig. 7). Basement membrane thickening started very early in Cy/+ rats (Fig. 9a) and consisted of multilaminated material which was increased in amount and usually partially surrounded the cysts (Fig. 9b). Focal basement membrane thickening was also occasionally found within glomeruli (Fig. 10). Thickened basement membranes were associated with an increase in immunoreactive type IV collagen and a marked increase in laminin (Fig. 11 a through d). Fibronectin immunoreactivity was increased in both the basement membrane and the interstitium in the established phase of the PKD (shown at 8 weeks of age in Fig. 11 e & f). By 24 weeks of age, kidneys from heterozygous male rats developed inflammatory infiltrates, consisting mainly of lymphocytes and macrophages; there was also interstitial fibrosis and increased interstitial collagen (Fig. 9c).

Renal proto-oncogene expression

Tubular epithelial cell proliferation is thought to be integral to cyst formation in PKD since individual tubule cell size does not increase in proportion to cyst surface area [10]. Increased abundance of proto-oncogene mRNAs has been observed previously in a murine model of autosomal recessive PKD [11, 12], perhaps reflecting an abnormality in cellular proliferation or

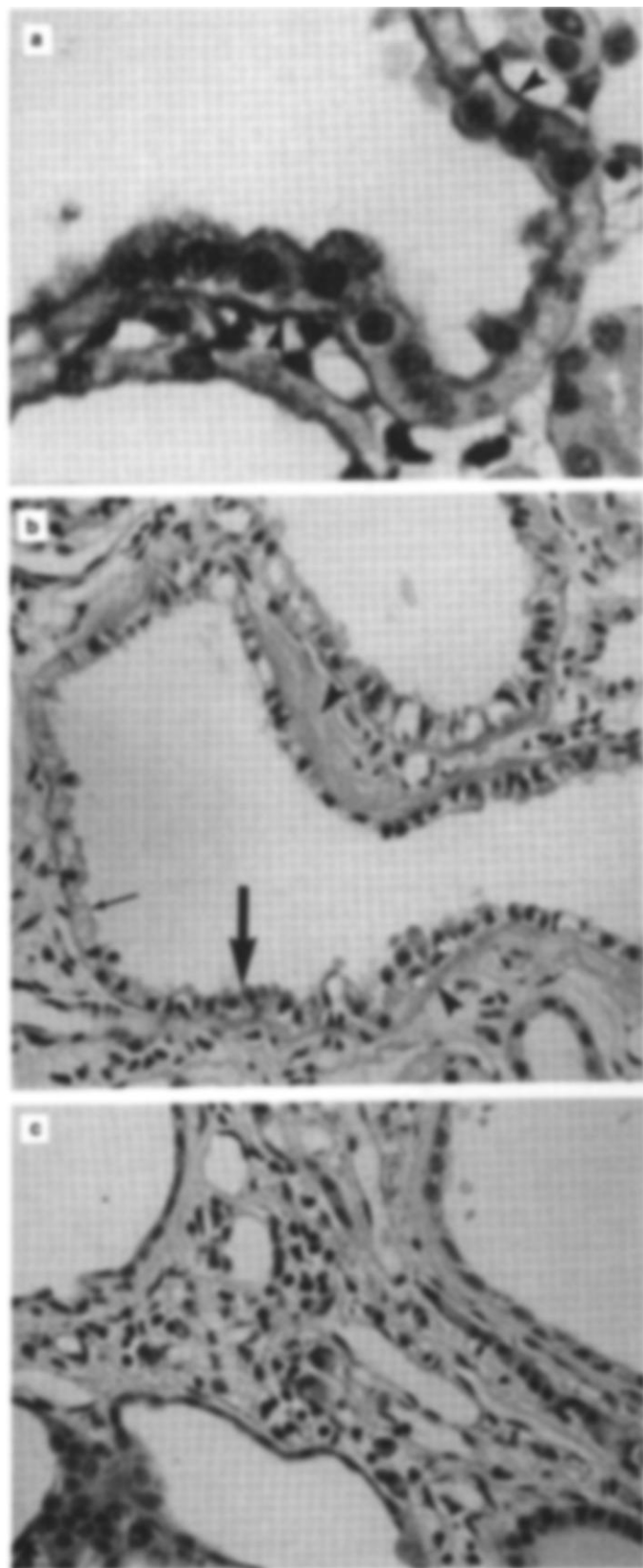


Fig. 9. Light micrographs of the extracellular matrix in kidneys from heterozygous *Cy/+* rats. (a) Focal basement thickening (arrowheads) was seen as early as 2 weeks of age and was associated with an increased packing density of cells and focal loss of brush border PAS staining. (b) Extensive areas of basement membrane thickening (arrowheads) were present in later stages of the disease. The cells overlying the thickened basement membrane (large arrow) appeared hyperplastic and showed loss of brush borders compared to more normal appearing proximal tubular cells in the same cyst (small arrow). (c) At 24 and 42 weeks, male heterozygous *Cy/+* rats exhibited significantly widened interstitial spaces with prominent infiltration by mononuclear leukocytes. (Magnifications: a 1,000 \times , b 320 \times , c 320 \times).

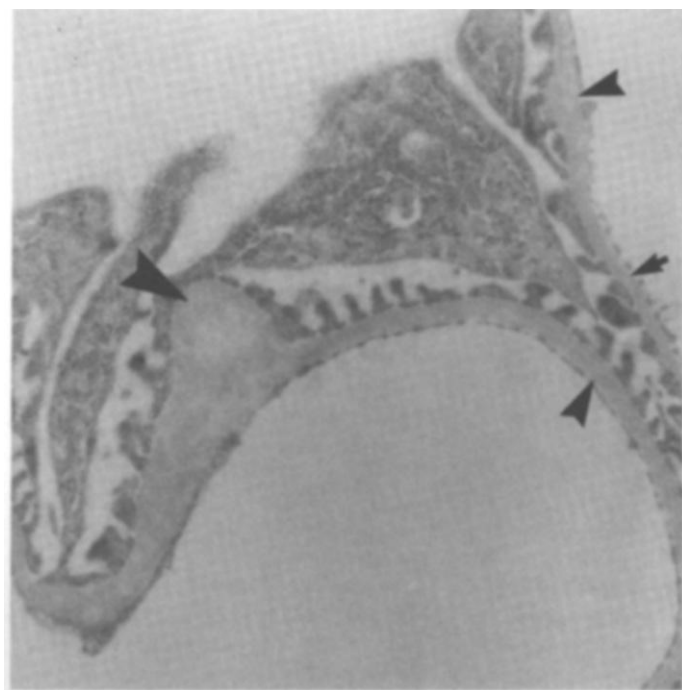


Fig. 10. Transmission electron micrograph of a glomerular loop from a 24-week-old male heterozygous *Cy/+* rat. Basement membranes of individual loops were diffusely thickened (small arrowhead) or exhibited large focal deposits (large arrowhead) as compared to relatively normal appearing basement membrane from an adjacent loop (arrow). (Magnification = 13,000 \times).

regulated during cell proliferation [7]. Renal *c-myc* levels in homozygous *Cy/Cy* rats were increased above normal littermate controls at two weeks and even more so at three weeks of age (Fig. 12). Renal *c-myc* levels were also elevated above control at 8 and 24 weeks of age in heterozygous *Cy/+* rats, which developed a more slowly progressive form of PKD.

To determine which cells in the kidney express *c-myc* mRNA, we performed *in situ* hybridizations in adult normal and *Cy/+* kidneys. Normal adult kidneys revealed levels of *c-myc* that were barely detectable (Fig. 13 a and b); however, kidneys from heterozygous *Cy/+* adult males, with pronounced cystic disease, expressed significant levels of *c-myc* in the epithelial cells lining cyst walls (Fig. 13 c and d).

Discussion

The current hypotheses for the pathogenesis of polycystic kidney disease rely on three features common to all forms of

cellular differentiation. To evaluate the role of abnormal cell growth in Han:SPRD rats, we determined the abundance in whole kidney of *c-myc* mRNA, a proto-oncogene that is

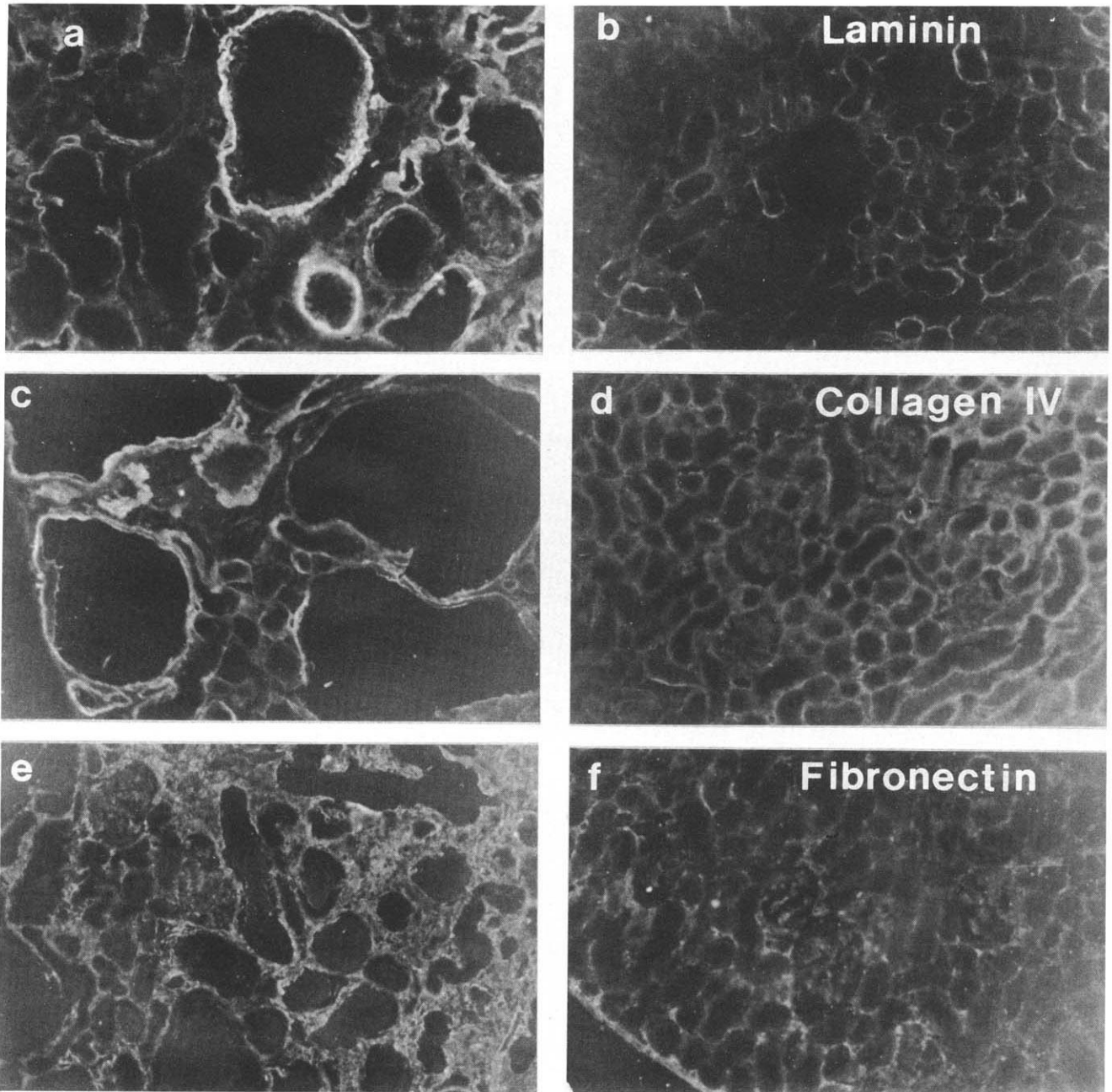


Fig. 11. Immunohistochemistry of kidneys from 8-week-old male normal $+/+$ (**b, d, f**) and heterozygous Cyl^{+} (**a, c, e**) rats stained for laminin (**a, b**), type IV collagen (**c, d**), and fibronectin (**e, f**). Thickened basement membranes of cysts stained very intensely for laminin (**a**) and moderately intensely for type IV collagen (**c**) as compared to normals (**b** & **d**). Fibronectin staining was more intense in the interstitium and basement membranes of cystic kidneys (**e**) compared to normal (**f**). All photographs are at the same magnification (300 \times).

this disease: (1) epithelial cell hyperplasia, (2) accumulation of fluid within cyst cavities, and (3) extracellular matrix abnormalities. Cyst expansion must be accompanied by increased numbers of epithelial cells lining the inner surface of cysts, since the size of individual cells does not increase with cyst growth [10]. The increased expression of proto-oncogenes in polycystic kidneys supports the supposition that epithelial cell proliferation is increased in PKD. The finding in the current study of increased expression of the *c-myc* proto-oncogene in the Han:SPRD rat model of autosomal dominant PKD, when viewed in

conjunction with similar findings in the C57BL/6J-*cpk* mouse [11, 12] and also in the DBA-*pcy* mouse (unpublished observations), demonstrates that elevated proto-oncogene expression is common to a number of different, spontaneously-occurring forms of PKD. The importance of epithelial proliferation and oncogene expression in PKD is further emphasized by the development of PKD in *c-myc* transgenic mice [13] and also in SV-40 large T antigen transgenic mice [14, 15]. Importantly, in Han:SPRD female heterozygotes, which manifested renal cystic disease but did not develop significant azotemia, there was

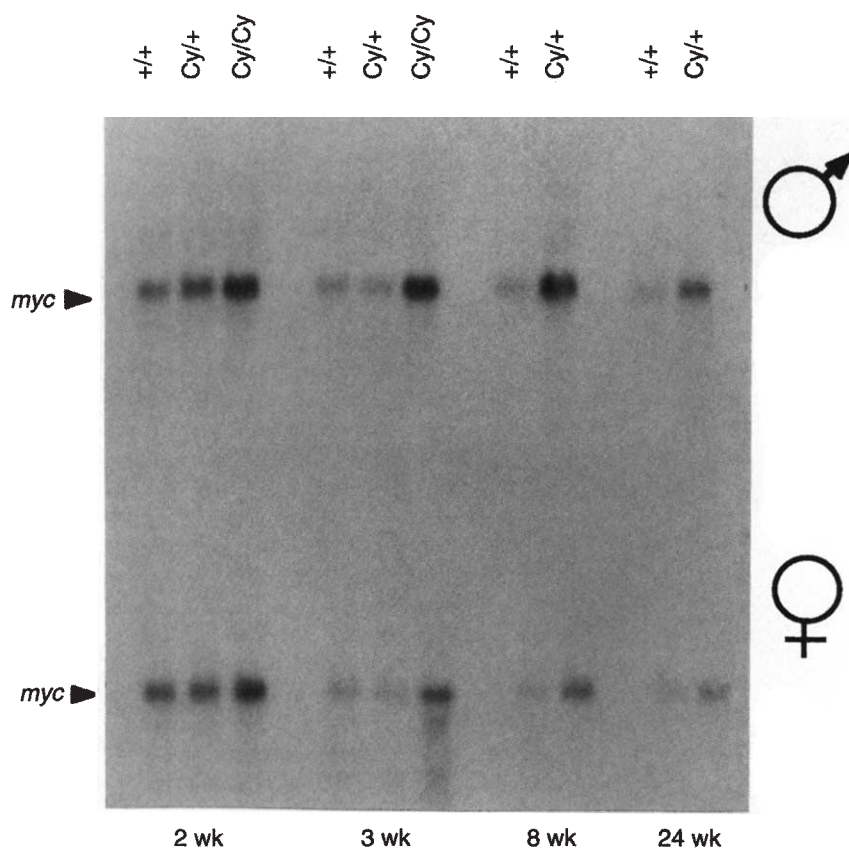


Fig. 12. *C-myc* mRNA levels in whole kidneys from normal $+/+$, heterozygous $Cy/+$, and homozygous Cy/Cy rats. Each lane contains 5 μ g of total cellular RNA. Samples shown are representative of all animals examined (see Methods). The upper row of lanes are from males and the lower lanes from females. Densitometry of all autoradiographs performed (Methods) revealed the following average signal intensities (normal $+/+$ signal is arbitrarily set equal to 1.0 at each age and for each sex; comparisons are only between animals of the same age and sex): 2 week old male ($+/+$ = 1.0, $Cy/+$ = 1.2, Cy/Cy = 1.8), 2 week old female ($+/+$ = 1.0, $Cy/+$ = 1.0, Cy/Cy = 1.4), 3 week old male ($+/+$ = 1.0, $Cy/+$ = 1.0, Cy/Cy = 4.1), 3 week old female ($+/+$ = 1.0, $Cy/+$ = 1.0, Cy/Cy = 4.7), 8 week old male ($+/+$ = 1.0, $Cy/+$ = 5.7), 8 week old female ($+/+$ = 1.0, $Cy/+$ = 3.4), 24 week old male ($+/+$ = 1.0, $Cy/+$ = 2.6), 24 week old female ($+/+$ = 1.0, $Cy/+$ = 1.9).

clearly elevated renal proto-oncogene expression (Fig. 12), consistent with a primary abnormality in the control of renal cell growth in PKD. Furthermore, in the Han:SPRD rat, proto-oncogene expression was clearly increased in cystic epithelium (Fig. 13), suggesting that there is a direct link between proto-oncogene expression and the development of renal cysts. In many systems, proliferation and differentiation appear to have a reciprocal relationship [16], perhaps explaining the finding of less-differentiated cellular phenotypes in the cells lining cysts (Figs. 6 and 7).

Expanding cysts must also remodel their physical environment as they enlarge. Altered extracellular matrix has been postulated to play a role in the pathogenesis of PKD [17]. While the abnormal basement membrane in PKD does not exhibit decreased tensile strength [18], evidence in other models suggests that cystic epithelial cells produce an abnormal basement membrane [19–21] and have an altered proliferative response to extracellular matrix proteins [21]. Abnormalities of the basement membrane surrounding cyst cavities were clearly evident in the Han:SPRD rat. There was focal basement membrane thickening (Figs. 7a, 7b, 9a, and 9b) and basement membranes appeared multilaminated by TEM (Fig. 7b). Several investigators have noted thickened and multilaminated basement membrane associated with cystic epithelia in human ADPKD [21, 22]. Glomerular basement membrane alterations, similar to those seen in $Cy/+$ rats (Fig. 10), are an early pathologic feature of human ADPKD [23]. Interestingly, the epithelial cells overlying areas of basement membrane thickening were atypical in

appearance, with a less-differentiated appearance (note the loss of apical brush borders in Figs. 7a, 9a, and 9b), an increased packing density, and an increased nuclear-to-cytoplasmic ratio, suggesting increased cell proliferation and partial dedifferentiation in these regions. This finding highlights the dynamic interaction between the epithelium and the basement membrane on which it rests. Since the basement membrane thickening was present in the earliest detectable cysts in heterozygous $Cy/+$ rats, a primary role for the basement membrane alterations in this model of PKD cannot be dismissed.

The etiology of renal failure in PKD is still a matter of debate. In homozygous Cy/Cy Han:SPRD rats, the rapid development of massive cystic disease without evidence of a significant inflammatory or fibrotic component suggests that the numerous, large cysts simply “crowd out” remaining normal nephrons, as expanding tumor masses distort parenchymal function. In contrast, whereas heterozygous $Cy/+$ males had a less aggressive progression of renal cystic disease, there was significant interstitial inflammation and fibrosis (Fig. 9) which was associated with renal dysfunction. Furthermore, heterozygous $Cy/+$ females developed a less aggressive renal cystic disease (Fig. 1 A and B) with minimal, if any, interstitial inflammation and fibrosis or, importantly, azotemia (Fig. 2B). These findings suggest that interstitial inflammation and fibrosis play an important role in the development in renal failure in the male Han:SPRD heterozygote. The presence of interstitial inflammatory cells also suggests that substances released by these cells (cytokines, lymphokines, chemotactic factors) may play a role

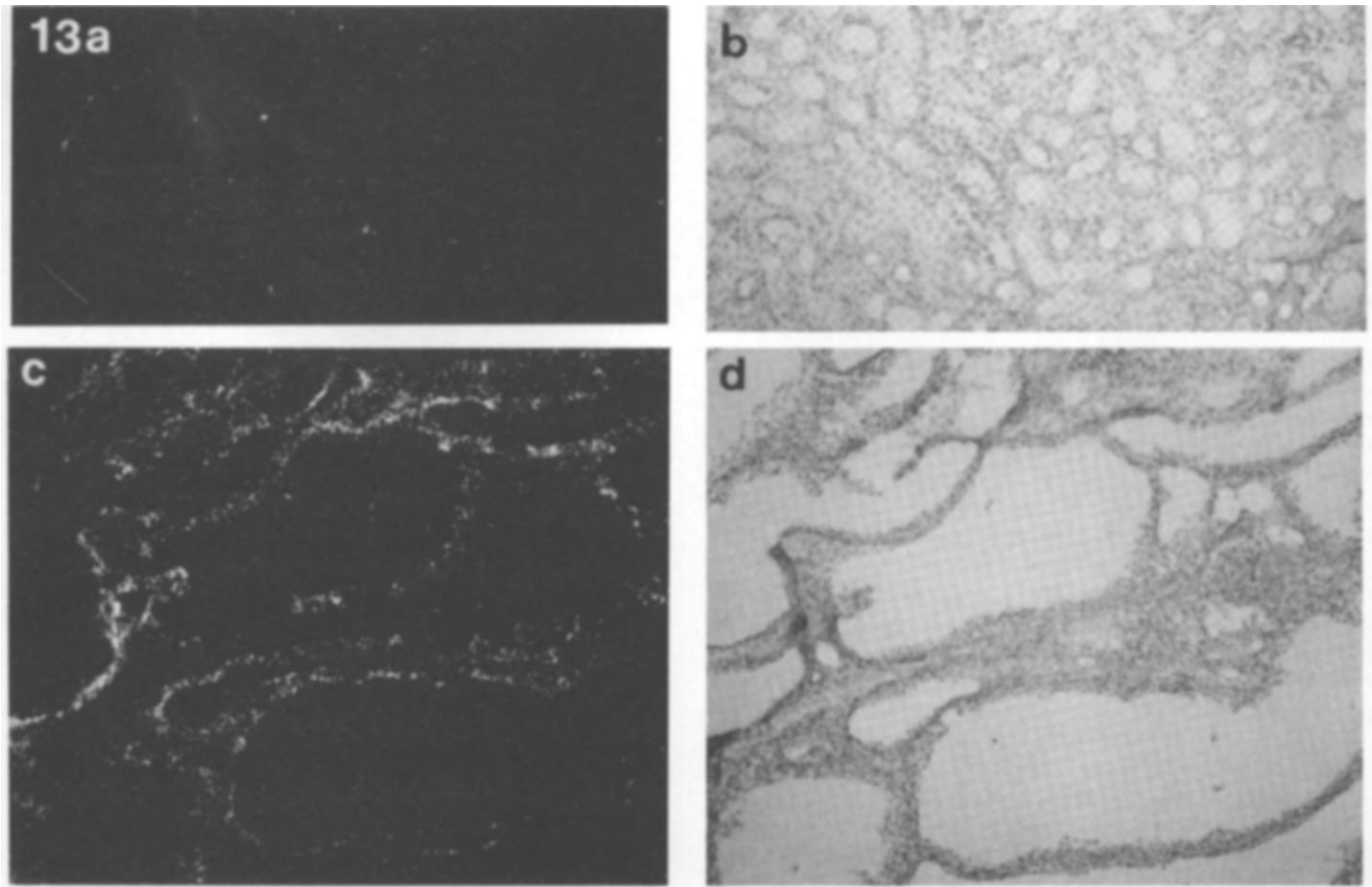


Fig. 13. *In situ* hybridization for *c-myc* mRNA in kidneys from 12-week-old male normal $+/+$ (**a**, darkfield, and **b**, brightfield) and heterozygous cystic $Cy/+$ (**c**, darkfield, and **d**, brightfield) rats. Normal kidney exhibits little autoradiographic labeling for *c-myc* mRNA, while the cystic kidney shows extensive hybridization localized primarily to the epithelia lining cyst cavities (**c**). All photographs are at the same magnification ($100\times$).

in the development of interstitial fibrosis in $Cy/+$ rats. Whether and how cysts trigger this interstitial response is unclear, but this process may involve an interaction of cysts with the interstitium and/or the elaboration of paracrine factors by cyst cells.

There is no discernible difference between sexes in the homozygous disease in this model. However, there is a striking difference in the renal disease manifested by male and female heterozygotes (Figs. 1 and 2). Both male and female heterozygotes develop renal cystic disease, however, only the males develop significant interstitial inflammation, interstitial fibrosis, and azotemia. Hormones unique to the respective sexes may affect the expression of the disease, but the specific cause of the more aggressive form of PKD seen in the males remains unexplained.

The potential utility of an animal model of any disease depends on how well it resembles aspects of the human condition. There are differences in the disease seen in the Han:SPRD rat and human ADPKD. Human ADPKD is associated with liver cysts, cerebral aneurysms, mitral valve prolapse, and colonic diverticuli [3]. To date, the extrarenal manifestations seen in the Han:SPRD are those seen in uremia and do not appear to be unique to the polycystic kidney disease [2]. In other respects, however, the Han:SPRD rat has several

features which resemble human ADPKD. As in human ADPKD, PKD in the Han:SPRD rat is inherited in an autosomal dominant fashion. By a strict definition, dominantly acting genes produce the same phenotype when present in heterozygotes or homozygotes; therefore, the Han:SPRD defect is not dominant in the strict sense. However, this may not reflect a difference from human ADPKD, since, to our knowledge, homozygous human ADPKD has not been reported. Human ADPKD is relatively common; consequently this lack of documented cases of homozygosity is perplexing. Homozygous human ADPKD may cause such profound anomalies in the kidneys (and possibly other organs) that fetuses cannot survive. PKD in the heterozygous Han:SPRD rat also resembles human ADPKD in its slow progression as well as its inheritance pattern. PKD in both the heterozygous Han:SPRD rat and human ADPKD is characterized by the development of cysts in all nephron segments; similar basement membrane abnormalities are also seen. Difference in the severity of cystic disease and the development of azotemia between male and female heterozygotes are also observed, although to a lesser degree, in human ADPKD [24].

The difference in the severity of cystic disease and the development of azotemia between male and female heterozygotes may make the Han:SPRD rat particularly useful in studies

of pathogenesis and treatment. Both male and female heterozygotes carry only one copy of the PKD gene, but there is a striking difference in the phenotypic manifestations which result. Thus the Han:SPRD rat serves to demonstrate that other factors can alter the expression of the primary genetic defect in PKD, and provides a model for examining the mechanisms involved in this type of epigenetic regulation of phenotype. The difference in the heterozygous disease between sexes also supports the hypothesis that therapy designed to alter the course of the disease may be possible. Specifically, in the Han:SPRD rat, administration of androgens may cause more aggressive PKD in female heterozygotes and castration (surgical and/or pharmacologic) may ameliorate the PKD seen in male heterozygotes. The association of renal interstitial inflammation and fibrosis with the development of azotemia in the heterozygous male Han:SPRD rat suggests that anti-inflammatory agents might also alter the progression of this disease. As more is learned about the pathogenesis of this disease, other therapeutic interventions will likely be suggested.

The Han:SPRD rat is the only well documented animal model of inherited PKD with an autosomal-dominant inheritance pattern and appears to have several features which resemble human ADPKD. The findings in the current study suggest the Han:SPRD rat will be a useful model for studies of the pathogenesis and treatment of inherited renal cystic disease.

Acknowledgments

The authors thank Dr. Kaspereit-Rittinghausen for generously providing the Han:SPRD rats used to found our colony. The authors also thank Dr. Jared Grantham for his instrumental role in obtaining these animals and for encouragement and helpful suggestions. This work was supported by Biomedical Research Support Grant #S07 RR05373 (BDC), Polycystic Kidney Research Foundation grants (BDC, VH), a grant from the American Heart Association-Kansas Affiliate (VH), and NIH grant DK37100 (JPC).

Reprint requests to Vincent H. Gattone, II, M.D., Department of Anatomy and Cell Biology, The University of Kansas Medical Center, 3901 Rainbow Blvd., Kansas City, Kansas 66160-7400, USA.

References

1. KASPAREIT-RITTINGHAUSEN J, RAPP K, DEERBERG F, WCISLO A, MESSOW C: Hereditary polycystic kidney disease associated with osteorenal syndrome in rats. *Vet Pathol* 26:195-201, 1989
2. KASPAREIT-RITTINGHAUSEN J, DEERBERG F, WCISLO A: Hereditary polycystic kidney disease: Adult polycystic kidney disease associated with renal hypertension, renal osteodystrophy, and uremic enteritis in SPRD rats. *Am J Pathol* 139:693-696, 1991
3. WELLING LW, GRANTHAM JJ: Cystic and developmental diseases of the kidney, in *The Kidney*, edited by BRENNER BM, Rector FC Jr, Philadelphia, W.B. Saunders, 1986, p. 1341
4. TAKAHASHI H, CALVET JP, DITTEMORE-HOOVER D, YOSHIDA K, GRANTHAM JJ, GATTONE VH, II: A hereditary model of slowly progressive polycystic kidney disease in the mouse. *J Am Soc Nephrol* 1:980-989, 1991
5. CHOMCZYNSKI P, SACCHI N: Single-step method of RNA isolation by acid guanidinium thiocyanate-phenol-chloroform extraction. *Anal Biochem* 162:156-159, 1987
6. THOMAS PS: Hybridization of denatured RNA and small DNA fragments transferred to nitrocellulose. *Proc Natl Acad Sci USA* 77:5201-5205, 1980
7. COWLEY BD JR, CHADWICK LJ, GRANTHAM JJ, CALVET JP: Sequential protooncogene expression in regenerating kidney following acute renal injury. *J Biol Chem* 264:8389-8393, 1989
8. DE SK, MCMASTER MT, DEY SK, ANDREWS GK: Cell-specific metallothionein gene expression in mouse decidua and placenta. *Development* 107:611-621, 1989
9. SALIDO EC, YEN PH, SHIPIRO LJ, FISHER DA, BARAJAS L: In situ hybridization of prepro-epidermal growth factor mRNA in the mouse kidney. *Am J Physiol* 256:F632-F638, 1989
10. GRANTHAM JJ, GEISER JL, EVAN AP: Cyst formation and growth in autosomal dominant polycystic kidney disease. *Kidney Int* 31:1145-1152, 1987
11. COWLEY BD JR, SMARDO FL JR, GRANTHAM JJ, CALVET JP: Elevated c-myc protooncogene expression in autosomal recessive polycystic kidney disease. *Proc Natl Acad Sci USA* 84:8394-8398, 1987
12. COWLEY BD JR, CHADWICK LJ, GRANTHAM JJ, CALVET JP: Elevated proto-oncogene expression in polycystic kidneys of the C57BL/6J (cpk) mouse. *J Am Soc Nephrol* 1:1048-1053, 1991
13. TRUDEL M, D'AGATI V, COSTANTINI F: c-myc as an inducer of polycystic kidney disease in transgenic mice. *Kidney Int* 39:665-671, 1991
14. MACKAY K, STRIKER LJ, PINKERT CA, BRINSTER RL, STRIKER GE: Glomerulosclerosis and renal cysts in mice transgenic for the early region of SV40. *Kidney Int* 32:827-837, 1987
15. KELLY KA, AGARWAL N, REEDERS S, HERRUP K: Renal cyst formation and multifocal neoplasia in transgenic mice carrying the SV40 early region. *J Am Soc Nephrol* 2:84-87, 1991
16. HARRIS H: The role of differentiation in the suppression of malignancy. *J Cell Science* 97:5-10, 1990
17. GABOW PA: Polycystic kidney disease: Clues to pathogenesis. *Kidney Int* 40:989-996, 1992
18. GRANTHAM JJ, DONOSO VS, EVAN AP, CARONE FA, GARDNER KD JR: Viscoelastic properties of tubule basement membranes in experimental renal cystic disease. *Kidney Int* 32:187-197, 1987
19. TAUB M, LAURIE GW, MARTIN GR, KLEINMAN HK: Altered basement membrane protein biosynthesis by primary cultures of cpk/cpk mouse kidney. *Kidney Int* 37:1090-1097, 1990
20. BEAVAN LA, CARONE FA, NAKAMURA S, JONES JK, REINDEL JF, PRICE RG: Comparison of proteoglycans synthesized by porcine normal and polycystic renal tubular epithelial cells in vitro. *Arch Biochem Biophys* 284:392-399, 1991
21. WILSON PD, HRENIUK D, GABOW PA: Abnormal extracellular matrix and excessive growth of human adult polycystic kidney disease epithelia. *J Cell Physiol* 150:360-369, 1992
22. CUPPAGE FE, HUSEMAN RA, CHAPMAN A, GRANTHAM JJ: Ultrastructure and function of cysts from human adult polycystic kidneys. *Kidney Int* 17:372-381, 1980
23. MILUTINOVIC J, AGODOA LCY, CUTLER RE, STRIKER GE: Autosomal dominant polycystic kidney disease. Early diagnosis and consideration of pathogenesis. *Am J Clin Pathol* 73:740-747, 1980
24. GRETZ N, ZEIER M, GEBERTH S, STRAUCH M, RITZ E: Is gender a determinant for evolution of renal failure? A study in autosomal dominant polycystic kidney disease. *Am J Kidney Dis* 14:178-183, 1989